

## Multi-objective Analysis of Multi-layered Core-shell Nanoparticles

Sawyer D. Campbell, Jogender Nagar, Pingjuan L. Werner, and Douglas H. Werner  
 Department of Electrical Engineering, The Pennsylvania State University  
 University Park, PA 16802, USA

### Abstract

Multi-layered spherical nanoparticles are known to be able to achieve large electric field enhancements via highly resonant electrically small geometries. While the resonant properties of these nanoparticles can be tailored by altering their material geometries, their scattered far-fields can subsequently be tailored as well. This is accomplished through a fortuitous superposition of electric and magnetic multipoles that yield the desired far-field patterns. In this study, the tradeoffs between traditional far field quantities, directivity and gain, are analyzed for a representative multi-layer configuration.

### 1. Introduction

Core-shell (*i.e.* “coated”) nanoparticles (CNP) have been extensively studied for their ability to achieve highly resonant behaviors in electrically small (*i.e.*  $ka < 1$ ) geometries [1]. This is achieved through the intelligent juxtaposition of epsilon-positive (EPS) and epsilon-negative (ENG) materials which facilitate the coupling of incident radiation into surface plasmon-polariton modes. Due to their strong field localization behaviors these CNPs have seen applications ranging from serving as vessels for localized drug-delivery [2] to nano-lasers [3]. While recently there has been much interest in these CNPs, analytical solutions for their scattering from plane wave sources have been known for over one hundred years [4]. Mie theory exploits the spherical symmetry of the particles to solve for the scattered field expansion coefficients for an arbitrary number of spherical layers of isotropic homogenous material composition. Interestingly, the scattering behavior of these CNPs can be greatly altered by their material parameters  $\epsilon$  and  $\mu$ , respective core/shell radii, and overall electrical size  $ka$ . While scattering by particles in the Rayleigh-limit (*i.e.*  $ka \ll 1$ ) is characterized by an electric-dipole mode, it is possible to achieve directional scattering or even minimize scattering [5] at desired angles for particles that are still considered electrically small. However, while the analytical theory exists, these solutions have to be found via thorough and exhaustive analysis for all but the simplest CNP configurations. Therefore, achieving arbitrary directional scattering patterns necessitates the application of advanced global optimization algorithms. In this paper, we investigate the size-dependent directivity and gain behaviors of a multi-layer CNP through the use of single- and multi-objective optimization algorithms.

### 2. Optimization of Multi-layer CNP

A depiction of plane-wave scattering by a multi-layer CNP is provided in Fig. 1.

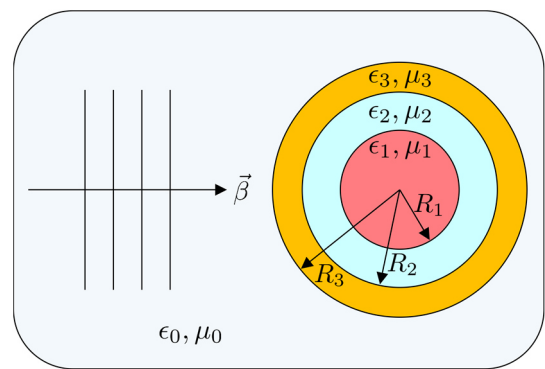


**Figure 1.** Plane wave scattering by a multi-layer core-shell spherical particle.

where  $\epsilon_i, \mu_i$ , and  $R_i$  are the constituent material parameters and radii of the CNP layers, respectively. A numerical implementation of Mie theory in Matlab is applied to solve for the scattered field expansion coefficients which govern the total scattered field via

$$\begin{aligned} \mathbf{E}_s &= \sum_{n=1}^{\infty} (ia_n \mathbf{N}_{e1n}^{(3)} - b_n \mathbf{M}_{o1n}^{(3)}) \\ \mathbf{H}_s &= \frac{-k}{\omega\mu} \sum_{n=1}^{\infty} (ib_n \mathbf{N}_{o1n}^{(3)} + a_n \mathbf{M}_{e1n}^{(3)}) \end{aligned} \quad (1)$$

where  $\mathbf{M}$  and  $\mathbf{N}$  are vector spherical harmonics and the superscript (3) indicates radial dependence on the spherical Hankel function of the first kind  $h_n^{(1)}$  [6]. Due to the completeness of this basis, any arbitrary scattering pattern can be generated. In practice, this means that the incident field must simultaneously excite all requisite modes with the proper weightings in the CNP to achieve the desired directional pattern. Furthermore, the magnitude of the multipole expansion coefficients governs the strength of the scattered field. When these coefficients are large and properly balanced, one can achieve both high scattered field directivity and gain. A scattered field directivity can be defined as

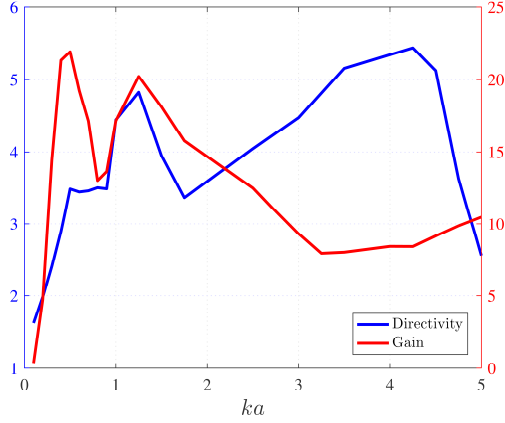


**Figure 2.** Directivity (blue) and gain (red) as a function of the particle size  $ka$  from a series of single-objective optimization runs.

$$D_s(\theta, \phi) = \frac{4\pi U_s(\theta, \phi)}{P_s} \quad (2)$$

where  $P_s$  is the total scattered power,  $U_s$  is the scattering intensity, and  $D_s$  is the directivity of the sphere relative to an isotropic scatterer. While the directivity relates to the shape of the far-field pattern, one is typically interested in how strong are the scattered fields and therefore we introduce the scattered gain

$$G_s(\theta, \phi) = e_s D_s(\theta, \phi) \quad (3)$$

where the scattered gain  $G_s$  is defined, in the usual way, as the product of the directivity and an efficiency factor  $e_s$ . For spherical scatters, one can formulate an efficiency as the ratio of the total scattered power relative to the total power that is incident onto the particle. This quantity is also proportional to the scattering cross-section in the following way:

$$e_s = \frac{P_s}{P_i} = \frac{C_{scat}}{\pi a^2} \quad (4)$$

where  $P_s$  is the total scattered power,  $P_i$  is the power incident upon the CNP,  $a$  is the particle's outer radius, and  $C_{scat}$  is the scattering cross-section of the particle. An interesting result of this formulation is that because electrically small particles can achieve scattering cross-sections many times greater than their geometrical cross-section [1], the scattering efficiency can therefore be much larger than unity. In traditional antenna terminology, the particle can have a pseudo aperture efficiency much greater than 100%.

To examine the directivity and gain behaviors, a series of single-objective optimization procedures were run. A four-layer particle was chosen for initial exploration and its material composition and interior radii ratios were optimized using CMA-ES [7-9]. The permittivity ( $\epsilon = \epsilon' + i\epsilon''$ ) was limited to  $-10 \leq \epsilon' \leq 10$  and  $0 \leq \epsilon'' \leq 10$  to capture a range of possible dielectric and plasmonic

materials. All materials are non-magnetic (*i.e.*  $\mu_r = 1$ ). In this study, the directivity and gain at the  $45^\circ$  polar angle were maximized in separate optimizations. A summary of the results is presented in Fig. 2. One can see that the peak gain and peak directivities occur at different  $ka$  values. This implies that there exists an immediate tradeoff between the two objectives. Interestingly, if both objectives were combined in a weighted sum, as is the standard practice, one may actually miss out on a portion of the solution space. Moreover, a single objective optimizer yields only a single solution and thus cannot provide any insight into the tradeoffs between competing objectives. However, a multi-objective optimizer produces a set of solutions, called the Pareto set, which is populated by points at which no further improvement in any objective can be realized without a simultaneous deterioration in all other objectives. Additionally, the analysis of the shape of the Pareto set, called the Pareto front, can be used to determine the tradeoffs between competing objectives. A multi-objective optimization of the same four-layer particle was then performed using Borg [10]. Three objectives were simultaneously optimized for performance at the same  $45^\circ$  polar angle: maximizing directivity and gain, and minimizing  $ka$ . A summary of the results is given in Fig. 3.

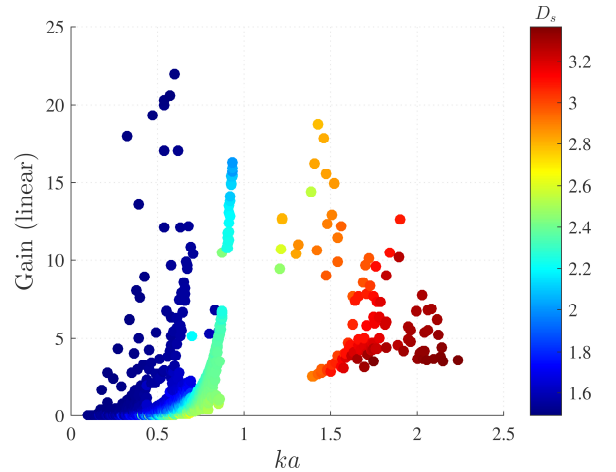


**Figure 3.** Pareto set from multi-objective optimization. Gain at the  $45^\circ$  polar angle is plotted against  $ka$ . The color is the directivity.

An interesting result of the analysis is that no particles larger than  $ka > 2.5$  were included in the Pareto set. This means that larger particles cannot achieve directivity or gain values that surpass those of the largest particle on the Pareto set. Another interesting result from the Pareto set is that there appears to be several families of solutions. Surprisingly, the largest gain values are achieved for particles around  $ka = 0.5$  in size. However, those particles have poor directivities. In fact, their directivity values indicate that these particles only excite electric dipole modes, albeit strongly. There also exist electrically small solutions that have higher directivities, but cannot achieve corresponding large values of gain. Finally, the largest

particles have the highest directivity values but there is a clear falloff in the gain that occurs as  $ka$  increases.

### 3. Conclusion

Through the use of a single-objective optimizer it was found that it was not possible to simultaneously maximize directivity and gain in a four-layer core-shell nanoparticle. Then a multi-objective optimization algorithm was employed to maximize both objectives and illustrate the tradeoffs between the two competing objectives while simultaneously minimizing the electrical size. While the particles studied in this paper were limited to a four-layer configuration, the number of layers can be included as an objective in future optimizations. Additional studies that are of interest include tradeoff analysis of directivity versus beamwidth and the inclusion of magnetic materials.

### 4. References

- [1] S. D. Campbell and R. W. Ziolkowski, "Impact of strong localization of the incident power density on the nano-amplifier characteristics of active coated nanoparticles," *Optics Communications*, vol. 285, no. 16, pp. 3341-3352, Nov. 2011.
- [2] Y. Chen, H. Chen, D. Zeng, Y. Tian, F. Chen, J. Feng, and J. Shi, "Core/shell structured hollow mesoporous nanocapsules: a potential platform for simultaneous cell imaging and anticancer drug delivery," *ACS Nano*, vol. 4, no. 10, pp. 6001-6013, Sep. 2010.
- [3] M. A. Noginov, G. Zhu, A. M. Belgrave, R. Bakker, V. M. Shalaev, E. E. Narimanov, S. Strout, E. Herz, T. Suteewong, and U. Wiesner, "Demonstration of a spaser-based nanolaser," *Nature*, pp. 1110-1112, Aug. 2009.
- [4] G. Mie, "Beiträge zur optik trüber medien, speziell kolloidaler metallösungen," *Annalen der Physik*, vol. 330, no. 3, pp. 377-445, 1908.
- [5] S. D. Campbell and R. W. Ziolkowski, "Simultaneous excitation of electric and magnetic dipole modes in a resonant core-shell particle at infrared frequencies to achieve minimal backscattering," *IEEE Journal of Selected Topics in Quantum Electronics*, vol. 19, no. 3, pp. 4700209-4700209, May-June 2013.
- [6] C. G. Bohren and D. R. Huffman, *Absorption and Scattering of Light by Small Particles*, Weinheim, Germany: Wiley-VCH Verlag GmbH, 1998.
- [7] N. Hansen and A. Ostermeier, "Completely derandomized self-adaptation in evolutionary strategies," *Evol. Comput.*, vol. 9, no. 2, pp. 196-195, 2001.
- [8] M. D. Gregory, Z. Bayraktar, and D. H. Werner, "Fast optimization of electromagnetic design problems using the covariance matrix adaptation evolutionary strategy," *IEEE Transactions on Antennas and Propagation*, vol. 59, no. 4, pp. 1275-1285, Apr. 2011.
- [9] M. D. Gregory, S. V. Martin, and D. H. Werner, "Improved electromagnetics optimization: the covariance matrix adaptation evolutionary strategy," *IEEE Antennas and Propagation Magazine*, vol. 57, no. 3, pp. 48-59, July 2015.
- [10] D. Hadka and P. Reed, "Borg: an auto-adaptive many-objective evolutionary computing framework," *Evolutionary Computation*, vol. 21, no. 2, pp. 231-259, May 2013.